Residual Stresses Measurement Around Welds By Optical Methods

PÁSTOR M.[1,a], HAGARA, M.[1,b], ČARÁK P.[1,c]

[1]Deparment of Applied Mechanics and Mechanical Engineering, Faculty of Mechanical Engineering, Technical University of Košice; 04200 Košice, Slovakia
[a]miroslav.pastor@tuke.sk, [b]martin.hagara @tuke.sk, [c]peter.carak@tuke.sk

Keywords: Residual Stresses, Welding Joints, Photostress, DIC

Abstract. The aim of this paper is the analysis levels of residual stress created by the welding process. The paper focuses on the evaluation of residual stresses. Residual stresses in welded structures affect the quality of the structure and therefore their quantification plays an important role. We can improve the mechanical properties of structures with the proper method of evaluation and with the help of suitable technology of removing residual stresses in welded joints, which can lead to increased durability and reliability of the structure. The residual stresses were evaluated using the hole drilling method with strain gauge rosettes, as well as the optical Photostress method using photosensitive coatings and digital image correlation (DIC).

Introduction

Among the most commonly used method for the permanent joining of materials is welding. It is widely used and is currently one of the preferred methods. Welded joints in structures present a certain risk because they can act as stress concentrators. The residual stresses introduced into the materials have a negative effect on the quality of the whole construction. At present, there is a great effort to evaluate residual stresses. The most common source of residual stresses is the machining of materials. Almost all machining technologies cause residual stresses in the workpiece. Another source of residual stresses may be the modification of the mechanical elements of the mechanism during its operation. In other cases, they may arise during installation of the element, assembly of the structure, occasional loading. According to its origin, the ways of residual stress formation can be divided into three categories, i.e. mechanical, temperature and metallurgical ones [1,2].

The cause may be one of these factors, or their combination, which results in residual stress. For example, during grinding, all three factors are combined (Fig. 1). The residual stresses in the structures can reach relatively high values. Especially if they are close to cracks, welds, cavities, etc. In these cases, residual stresses are difficult to observe and can cause damage at a lower load than the maximum permissible load. [3].
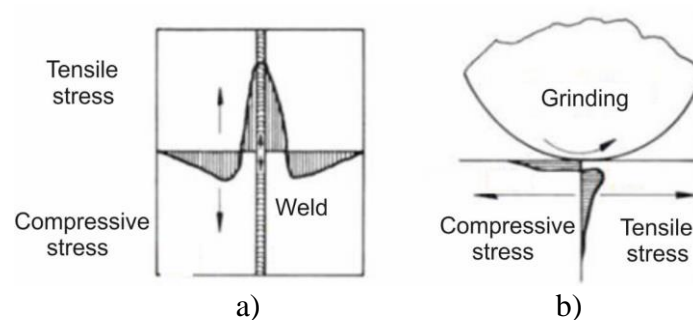
a)   b)
Fig. 1: Residual stress created by a) welding and b) grinding [3]

Fastening technology is a very important part of the industry. Welding of metals is the best known and most commonly used connection technology [4]. During welding three distinct areas are formed, i.e.: the weld metal to be melted, the heat affected area that undergoes the thermal cycle of the welding process, and the parent metal that is unaffected during the operation. By applying post-weld heat treatment, the material properties can be adjusted to the desired, but the temperature changes induced by the welding result in undesirable effects on the original microstructure, meaning a deviation of the mechanical properties in and around the weld from the material not affected by welding (Fig. 2). This represents a number of possibilities in terms of the generation of undesirable residual stress [4].
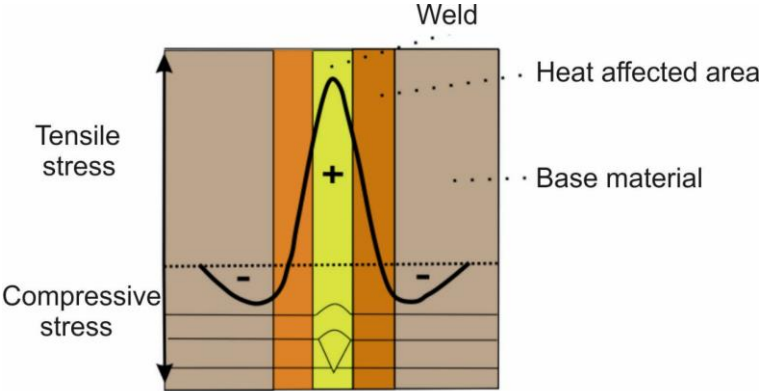
Fig. 2: Distribution of residual stresses created by welding

Welding is a process that is based on local heat generation by a moving heat source. The material to be welded reaches the melting point very quickly and then cools down rapidly causing microstructural and mechanical changes in properties and creating residual stresses [5].

The residual stresses present in the workpiece are the result of uneven expansion and compression of the weld and the base material due to the uneven heat distribution during the welding process. Usually, the residual stresses recorded in the weld joints are tensile and have a negative effect on the welded components. On the other hand, the residual compressive stresses can have beneficial effects on welded material. Tensile residual stresses can cause cracks, while compressive stresses can improve component quality. Tensile stresses are generated as a result of material shrinkage, while compressive stresses are generated by hardening and phase transformation. Both types of stresses exist in the weld joint, but their distribution depends on the position of the weld. The properties of a welded joint structure can be improved by applying specific processing to a particular location depending on residual stress distribution data. Fort that reason it is important to identify the weld residual stresses and their distribution to improve the quality and reduce the negative effects in the welded components [5].

Evaluation of Residual Stresses

Detecting and measuring residual stresses is important in predicting the life of a component or structure, analysing deformations and detecting failure reasons. All measurement techniques are divided into non-destructive, semi-destructive and destructive (see Table 1). The choice of a measurement method depends largely on the information we need to obtain about the specimen. An important aspect of such measurements is the knowledge of each measurement technique, their possibilities and limitations [6].

In practice, the determination of residual stresses in structures and machine components is usually based on the hole-drilling method. This method has the advantages of high accuracy and reliability, a standardized measurement process and appropriate practical application. This

is a semi-destructive method because in most cases the drilled hole is very small in comparison to the specimen size. The drilled hole is often also repairable or negligible [7]. Strain gauge rosettes are used for recording relaxed deformations by hole drilling from which residual stresses are calculated [8].

Table 1: Distribution of methods by the destruction

Non-destructive method	Semi-destructive method	Destructive method
Barghausen noise	Hole drilling method	Partitioning method
RTG diffraction	Ring-Core method	Contour method
Neutron diffraction		
Ultrasonic method		

The strain gauge rosette differs from the classical strain gauge in that it has three measuring grids. Their position and rotation relative to each other on the rosette are precisely defined. Using a conventional drilling method, a hole is drilled into the centre of the rosette and deformations are measured in the material around. By the Ring-Core method, deformations are measured at the centre of the strain gauge while drilling is carried out around the rosette, where the annular groove is drilled. In Fig. 3, these methods are schematically illustrated, where D_0 is the diameter of the drilled hole and D is the mean diameter of the rosette [5]. H expresses the maximum hole depth if the measurement is still quantifiable, and ε_1, ε_2, ε_3 represent the relaxed deformations on the strain gauge sensors [8].

The Ring-Core method has the advantage of greater relaxed deformations. Nevertheless, in most cases, the conventional hole drilling method is used because of ease use and less damage to the specimen during drilling [7].
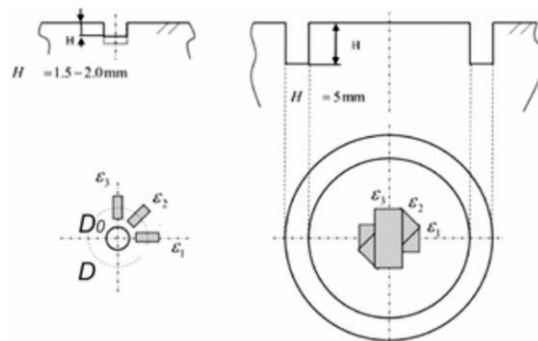
Fig. 3: Methods for measuring residual stresses with strain gauges, a) conventional hole drilling method, b) Ring-Core method

The scheme for investigating the released strains at any point of plane stress is shown in Fig. 4 [9].
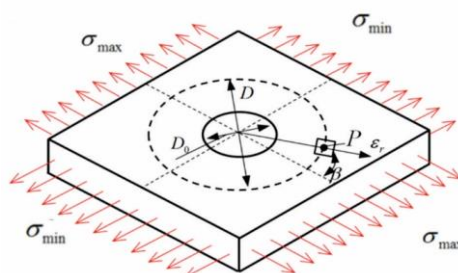
Fig. 4: Investigation of relaxed deformations at any point of plane stress

The general expression for the released relative radial deformation at the point, in the case of biaxial residual stress, can be expressed by

$$\varepsilon_r = (\bar{A} + \bar{B}\cos2\beta)\sigma_{max} + (\bar{A} - \bar{B}\cos2\beta)\sigma_{min} \qquad (1)$$

where ε_r is the represents the released deformation in the radial direction registered by the strain gauge centered at point P, $\bar{A}, \bar{B}$ are the calibration coefficients, β is the angle measured counterclockwise from the direction of the strain gauge to the direction σ_{max}, σ_{max} is the maximum normal stress at the hole before drilling, σ_{min} is the minimal principal normal stress at the hole before drilling, D is the mean diameter of the strain gauge rosette and D_0 is the hole diameter [10].

The coefficients $\bar{A}, \bar{B}$ are obtained empirically, it is by experimental calibration or numerical modelling using FEM. When introducing another independent variable - dimensionless hole depth, the generalized form of functions for coefficients can be expressed by

$$\bar{A} = f_A(E, \mu, r, Z/D)$$
$$\bar{B} = f_B(E, \mu, r, Z/D).$$

The procedure for measuring and evaluating the residual stresses have been described in standard ASTM E837-13a [11]. In the drilling method, it is necessary to recognise what type of specimen we use. We distinguish between "thin" and "thick" specimens. A specimen can be considered "thick" if its thickness is at least 1.2 D. When drilling such a specimen, the blind hole principle is applied, the drilling is performed in-depth increments. After each measurement step the strain gauge sensor records the relaxed deformations ε_1, ε_2, ε_3. According to standard ASTM E 837-13a, the measurement should be performed to a maximum depth corresponding to a ratio $Z/D = 0.4$, where the constant Z represents the depth of the hole and the constant D represents the mean diameter of the strain gauge rosette. A specimen of less than 0.4 D thick is considered to be 'thin'. In this case, the measurement is performed simultaneously, without increments. This rule for the through-hole applies, which means that the specimen is drilled in one step and only one strain relief value is obtained from all strain gauge sensors ε_1, ε_2, ε_3 [3].

Experimental determination of residual stresses near welded joints

The experimental part was focused on the verification of residual stresses near the weld joint by using optical methods as well as the hole drilling method. The aim was to compare residual stresses at individual sites of the test specimen, close and outside of the weld joint. This comparison determined the distribution of residual stresses at individual locations near and outside the weld joint.

First of all, the chemical composition of the specimen was determined, and based on the obtained data it was determined that the material was S235J2 with a thickness of 13 mm. The material characteristics required for the experiment are determined by the elastic modulus $E = 200$ GPa, Poisson's ratio $\mu = 0.3$, ultimate strength $R_m = 360$-510 MPa and upper yield point $R_{eH} = 235$ MPa. The weld joint was made by electric arc welding with a melting electrode E-R 117 (Fig. 5).

Fig. 5: Tested specimen

Fig. 6 shows the locations of the measurement points on the evaluated specimen.
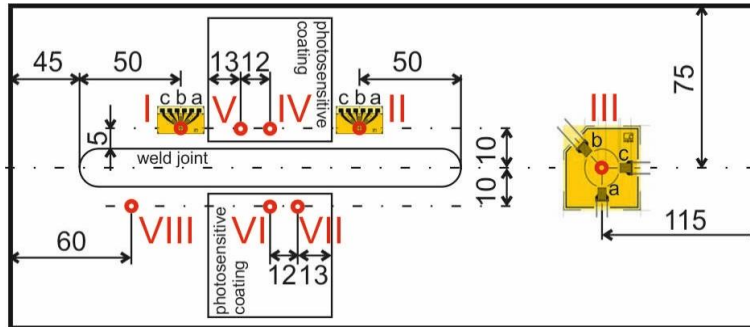
Fig. 6: Locations of the measurement points

As can be seen in Fig. 1, high tensile stresses are located 10 to 20 mm from the center of the weld joint. For this reason, the distance from the center of the weld joint was 10 mm (approximately 5 mm from the weld edge). Eight measurement points were selected for comparison (Fig. 6). Two of them (I and II) using strain gauges near the weld edge, each 50 mm from the ends of the weld joint and two photosensitive coatings between them with drilled holes (IV to VII), which were evaluated by Photostress. The hole VIII was drilled near the weld joint 60 mm from the edge of the specimen and evaluated by the DIC method. Location III was selected outside of the affected area to compare drilling data without interfering residual stresses generated by welding to the results. Three drilling devices were used in the experiment. It was a high-speed drilling device SINT MTS 3000 (Fig. 7), a high-speed and low-speed drilling device RS-200 (Fig. 8). Finally, a prototype of a device enabling the evaluation of released strains in individual steps of drilling by optical methods was also tested (DIC, Photostress) (Fig. 9). The P3 data bus was used for RS-200 measurements. The P3 reads the strain values during the RS-200 measurement at low speed, high-speed drilling.
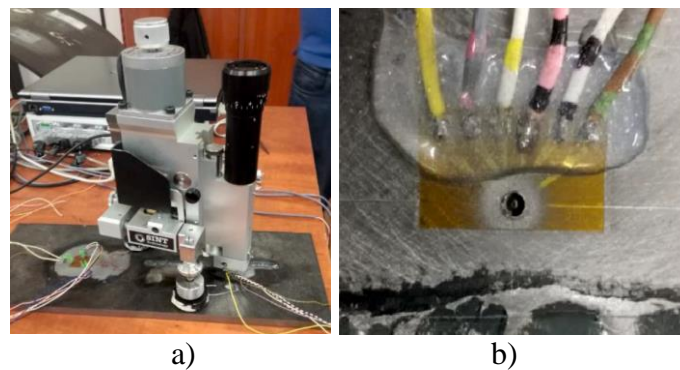
a)   b)
Fig. 7: Drilling device SINT MTS 3000 a) whole view b) detail of the measured point

<div align="center">a)   b)</div>
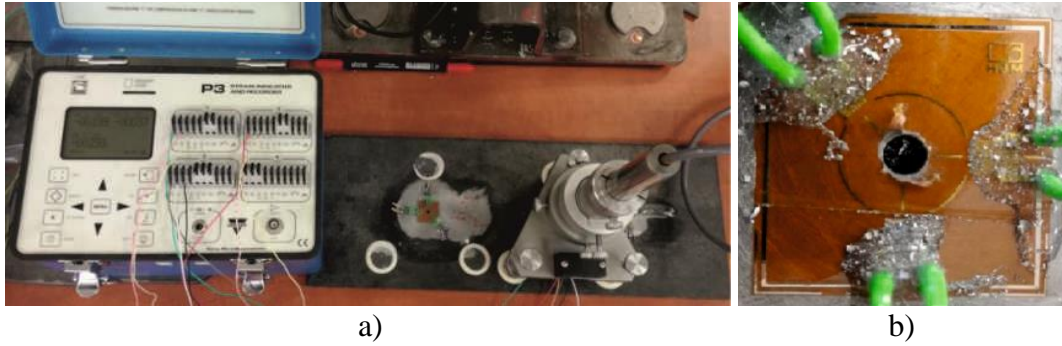
Fig. 8: RS-200 drilling device and P3 data bus a) whole view b) detail of the measured point

After drilling the specimen at eight measuring points, we obtained the values of released deformations, from which were evaluated the residual stresses in selected locations. The residual stress values obtained by drilling with SINT MTS 3000 and RS-200 are given in (Table 2). The angle α was measured from the grid *a* of strain gauge rosettes (see Fig. 6).

<div align="center">a)   b)</div>
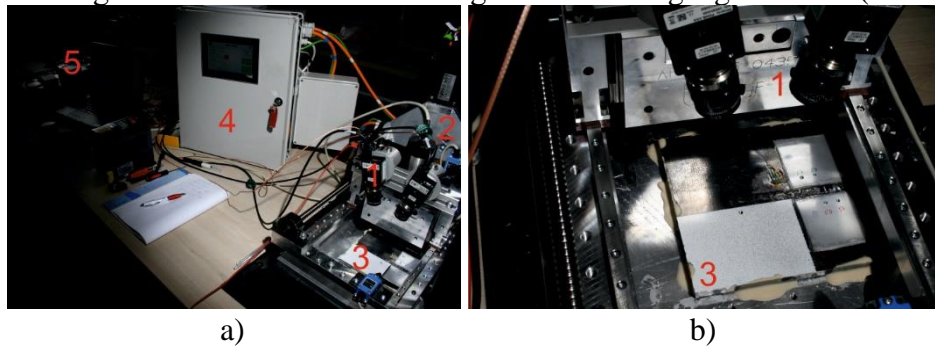
Fig. 9: Drilling device using Photostress and DIC methods to quantify residual stresses by standard ASTM E 837-13a, where 1 couple of DIC cameras with high definition, 2 drilling device, 3 specimen, 4 control unit, 5 measuring and evaluating device a) whole view b) detail of the measured point

<div align="center">Table 2: The values of residual stresses reached by the hole drilling method</div>

Hole Drilling Method			
Location	σ_{min} [MPa]	σ_{max} [MPa]	α [°]
I	145,67	563,37	-45,33
II	169	388	-51
III	15	10	-79

The SINT MTS 3000, RS 200 and the newly designed drilling device were used to compare the measurements near the weld joint. For measurements near the weld joint was used the strain gauges type RY61 from the manufacturer HBM. From the measured deformations, it is possible to assume tensile residual stress at the places near the weld joint, because the values of released strains were negative. For reference measurements outside the weld area, the measurement was performed with the RS-200 hand drilling device and the strain gauge type RY21. The measured deformations at this point were positive, indicating that there were compressive residual stresses at the drilling point.

Because the workplace has extensive experience using experimental methods in practical tasks, the results of experimental measurements of residual stress determination by drilling method were verified by optical methods Photostress and DIC. It should be noted that the use of optical methods (DIC, ESPI) in combination with drilling is solved by several authors [12-16]. The advantage of these non-contact methods is, among other things, the possibility of full-field analysis in the research area.

The experimental measurement procedure for the Photostress method was used to evaluate the specimen with applied optically sensitive coating Vishay PS-1D. In Fig. 10 there is a view of a specimen with an applied coating. For a "rough" comparison of the results, was drilled 3.2 mm blind hole to a depth 0.5 mm and 1.5 mm on both sides of the specimen. A newly designed drilling device was used for drilling (Fig. 11). Fig. 12 shows the locations where residual stress values have been read. Measured points have been chosen on the edge of drilled holes close to the weld joint because residual stresses were measured as close as possible to the weld joint.
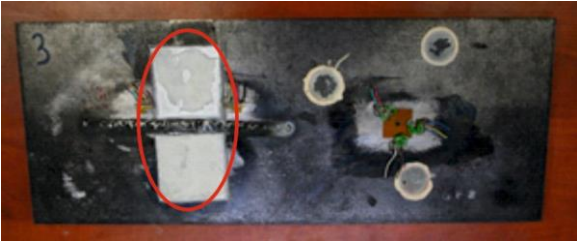
Fig. 10: Specimen with applied photosensitive coatings
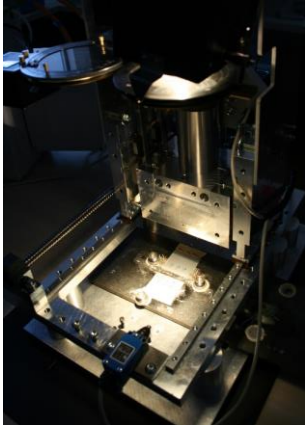
Fig. 11: Newly designed drilling device with Photostress module
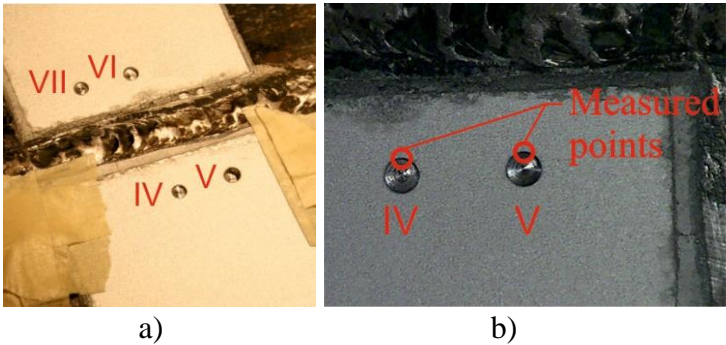
a)   b)
Fig. 12: Location of the examined points on the specimen a) position of drilled blind hole b) detail of examined points at the edge of the drilled blind hole

After drilling the blind hole, one point was selected as close as possible to the weld joint on each drilled hole (see Fig. 12b). To determine the stress levels at the examined points, it was necessary to measure the corresponding fringe order from the compensator. The process of measuring the fringe order using a compensator is shown in Fig. 13. The comparison of the initial and final state during measuring the fringe order is shown in Fig. 14. According to the orientation of the compensator at the investigated point on the edge of the blind hole, it is possible to determine whether it is tensile resp. compressive stresses. On the edge of the hole,

one of the main stresses is equal to zero and therefore the non-zero stress is determined from the relation

$$\sigma = \frac{E}{1+\mu} \cdot N \cdot f \tag{2}$$

where N is the line order, f is the photosensitive constant, μ is the Poisson's ratio and E is Young's modulus of elasticity.

<div align="center">a)   b)</div>
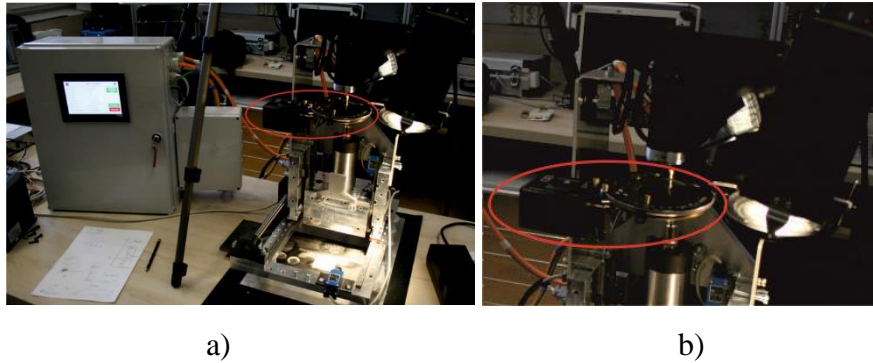
Fig. 13: Measuring the fringe order using a compensator a) whole view, b) detail view

<div align="center">a)   b)</div>
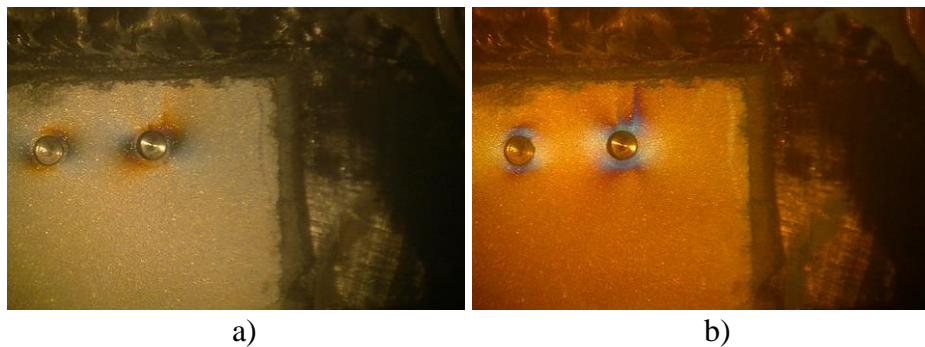
Fig. 14: The process of measuring a fringe order a) initial state b) final state

In Table 3 shows the measured fringe orders using the compensator as well as the depths of the individual holes, the directions and the resulting values of the stresses at the individual locations.

<div align="center">Table 3: Values of residual stresses measured by Photostress</div>

Location	Depth [mm]	Orientation of compensator	Fringe order N [-]	Stress value σ Photostress [MPa]
IV	0,5	=	0,5	291
V	1,5	=	0,59	344
VI	0,5	=	0,36	210
VII	1,5	=	0,56	326

Based on the results obtained by the Photostress method, it can be stated that in measured locations were tensile stresses thus negative residual stresses.

The experimental measurement process for the DIC method is based on applying a stochastic pattern to a specimen near the weld joint. In Fig. 15 there is a view of a specimen with a created

pattern and a drilled hole near the weld joint. To compare the results was drilled a 3.2 mm blind hole to a depth of 2 mm and 10 mm from the edge of the weld joint. Drilling was performed using a newly designed drilling device.

a)   b)

Fig. 15: Specimen with the applied stochastic pattern a) whole view, b) hole drilled near the weld joint

The reference images with 2452x2056px resolution (pixel density ca. 53px/mm) captured by the 3D DIC system Q-400 Dantec Dynamics can be seen in Fig. 16. As the results of strain analysis performed by the DIC method, which are used to calculate the residual stresses due to the standardized methodology, mentioned in ASTM E 837-13a, were markedly affected by the noise and did not correspond to the results obtained by strain gage as well as Photostress method. The successive change of displacement X and Y, respectively, during the hole-drilling obtained by 3D DIC system Q-400 Dantec Dynamics is depicted in Fig. 17.
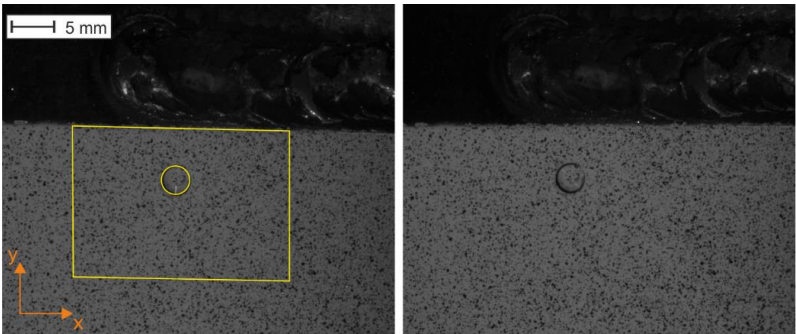
Fig.16: Reference images captured by the 3D DIC system Q-400 Dantec Dynamics with depicted evaluation mask
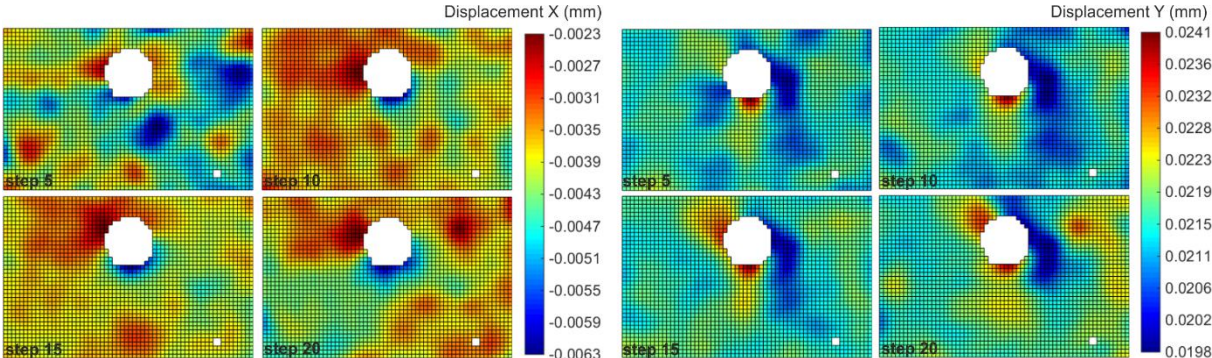
Fig.17: Successive change of displacement X and Y, respective, obtained during the hole-drilling by DIC

Due to obtained results from DIC affected by the noise, the authors' plan is to propose a methodology to compute the residual stresses from the obtained displacements.

Conclusions

The paper presents the procedure of experimental measurement on specimen with welded joint using three experimental methods. However, as already mentioned at the beginning of the paper, welded joints in structures present a certain risk because they can act as stress concentrators. Due to the negative effect of the welds on the structure, it is necessary to consider the possibilities of reducing these stresses. For this reason, identifying the weld residual stresses and their distribution is important to improve the quality and reduce the negative effects in the welded components. From the results obtained from drilling and the Photostress method can be found tensile residual stresses in the investigated area, which is consistent with theoretical assumptions. Due to results from DIC affected by noise, the authors plan methodology for computing the residual stresses from displacement.

Acknowledgments

References

[1] Residual Stress., Integration de la notion des. Online:

[2] R. Nedin, V. Dudarev, Some aspects of modeling and identification of inhomogeneous residual stress, Engineering Structures, 151, (2017), 391-405

[3] Micro-Measurement Vishay Precision Group, Measurement of Residual Stresses by the Hole-Drilling* Strain Gage Method, Tech Note TN-503, (2010), 19-34

[4] W. Rae, Z. Lomas, Measurement of residual stress and microstructural evolution in electron beam welded Ti-6Al-4V using multiple techniques, Materials Characterisation, 132, (2017), 10-19

[5] N. Nadhira, M. Sarizam, Review on Welding Residual Stress, ARPN Journal of Engineering and Applied Sciences, 9, (2016), 6166-6175

[6] D. Walker, Residual Stress Measurement Techniques, Advanced Materials & Processes, (2001), 30-33

[7] G. S. Schajer, Hole drilling Residual Stress measurement at 75: Origins, Advancer, Opportunities, Experimental Mechanics, 50, (2010), 245-253.

[8] M. Steinzig, D. Upshaw, J. Rasty, Influence of Drilling Parameters on the Accuracy of Hole-Drilling Residual Stress Measurements, Experimental Mechanics, 54, (2014), 1537-1543

[9] A. S. Kobayashi, Handbook on Experimental Mechanics, Society for Experimental Mechanics, Vch Pub, 1993.

[10] G. S. Schajer, Practical residual stress measurement methods, John Wiley & Sons Ltd, 2013.

[11] ASTM E 837-13a: Standard Test Method for Determining Residual Stresses by the Hole-Drilling Strain-Gage Method.

[12] Y. Min M. Hong Z. Xi L. Jian, Determination of residual stress by use of phase-shifting moiré interferometry and hole-drilling method, 44, (2006), 68-79

[13] G. S. Schajer, Application of Finite Element Calculations to Residual Stress Measurements, Journal of Engineering Materials and Technology, 103, (1981), 157-163

[14] M. Hagara, F. Trebuňa, M. Pástor, R. Huňady, P. Lengvarský, Analysis of the aspects of residual stresses quantification performed by 3D DIC combined with standardized hole-drilling method, Measurement, 137, (2019), 238-256

[15] E. Ponslet, M. Steinzig, Residual Stress Measurement Using the Hole Drilling Method and Laser Speckle Interferometry. Part II: Analysis Technique, 27, (2003), 17-21

[16] G. S. Schajer, M. Steinzig, Full-field calculation of hole drilling residual stresses from electronic speckle pattern interferometry data, Experimental Mechanics, 45, (2005), 526-532